Cell Biochemistry and Biophysics
https://doi.org/10.1007/s12013-020-00949-8

ORIGINAL PAPER

In Silico Prediction of Metabolic Fluxes in Cancer Cells with Altered S-adenosylmethionine Decarboxylase Activity

Olga Dotsenko[1] · Dmytro Shtofel[1,2]

Accepted: 28 September 2020

Abstract
This paper investigates the redistribution of metabolic fluxes in the cell with altered activity of S-adenosylmethionine decarboxylase (SAMdc, EC: 4.1.1.50), the key enzyme of the polyamine cycle and the common target for antitumor therapy. To address these goals, a stoichiometric metabolic model was developed that includes five metabolic pathways: polyamine, methionine, methionine salvage cycles, folic acid cycle, and the pathway of glutathione and taurine synthesis. The model is based on 51 reactions involving 57 metabolites, 31 of which are internal metabolites. All calculations were performed using the method of Flux Balance Analysis. The outcome indicates that the inactivation of SAMdc results in a significant increase in fluxes through the methionine, the taurine and glutathione synthesis, and the folate cycles. Therefore, when using therapeutic agents inactivating SAMdc, it is necessary to consider the possibility of cellular tumor metabolism reprogramming. S-adenosylmethionine affects serine methylation and activates serine-dependent de novo ATP synthesis. Methionine-depleted cell becomes methionine-dependent, searching for new sources of methionine. Inactivation of SAMdc enhances the transformation of S-adenosylmethionine to homocysteine and then to methionine. It also intensifies the transsulfuration process activating the synthesis of glutathione and taurine.

Keywords Metabolic flux · S-adenosylmethionine decarboxylase · Stoichiometric model · Polyamine metabolism · Flux balance analysis · Cancer cell

Introduction

Numerous reactions of methylation in cells, including rearrangement of methyl groups on histone tails, methylation of DNA cytosine and mRNA adenine, require S-adenosylmethionine (SAM) as a donor of methyl groups. SAM is a product of a single-carbon metabolic pathway and is involved in the catabolism of serine. Many works indicate that histone and DNA methylation reactions are sensitive to the concentration of SAM [1–3]. Alongside, spermine, spermidine, and other polyamines are created from the decarboxylated form of SAM and putrescine [4, 5]. Since polyamines are directly involved in cell activity, the studies focus on the role of these substances in malignant growth [1, 6]. The relations between polyamines and cancer have been investigated for many decades, resulting in extensive and comprehensive studies on enzymes and metabolic pathways. Consequently, many chemotherapy strategies for cancer were based either on inhibiting the synthesis of polyamines or on activating their catabolism. The metabolism of polyamines in tumor growth is a good example of interaction between genes and metabolites, since specific oncogenes and tumor suppressors control the metabolism of polyamines, and their concentration affects the rate of cell proliferation [1, 5, 7, 8].

The increased biosynthetic flux of polyamines dramatically increases the demand for the metabolic pathways of carbohydrates, methionine, and folates, which begin to increase the metabolite production in order to maintain nucleotide and SAM pools [1, 2, 9, 10].

The major polyamine biosynthesis enzymes are pyridoxal-5-phosphate-dependent ornithine decarboxylase (ODC) and pyruvate-dependent S-adenosylmethionine decarboxylase (SAMdc). Spermine/spermidine-N1-acetyltransferase (SSAT)

✉ Dmytro Shtofel
shtofel@vntu.edu.ua

[1] Department of Biophysics and Physiology, Vasyl' Stus Donetsk National University, 600-richchia str. 21, Vinnytsia 21021, Ukraine

[2] Department of Biomedical Engineering, Vinnytsia National Technical University, Khmelnytske Shose 95, Vinnytsia 21021, Ukraine

Published online: 11 October 2020

plays the main role in the catabolism of polyamines. The biosynthesis of these enzymes is subtly controlled at the transcriptional and translational levels. The basic principles of this regulation are now established for both normal and tumor cells.

Creating the specific inhibitors for enzymes of polyamine biosynthesis and catabolism was one of the main goals of polyamine biochemistry for a long time [1, 11–13]. However, the most therapeutic strategies based on specific inhibition of the key metabolic enzyme have not been successful, presumably due to the presence of compensatory mechanisms of polyamines metabolism, which buffer the effects induced by an impact on a particular enzyme. Another reason is the redistribution of fluxes in metabolic pathways, which contribute to the further growth of the tumor.

Changes in the metabolism of cancer cells can directly affect epigenetic regulation and facilitate its transformation. Serine can contribute to this process by supplying carbon units for the regeneration of methionine from homocysteine (HCY) through the de novo ATP synthesis [14–16]. The importance of folate-mediated carbohydrate metabolism for cancer cells proliferation has been long assessed [17], and is being studied until present [10, 14–16, 18, 19]. Serine plays a key role in the transfer of carbon units to the tetrahydrofolate (THF), supporting nucleotides synthesis and NADPH production. Cancer cells have a high demand for serine, and its pool is supported by exogenous absorption and de novo synthesis from glucose [3, 14–17]. The enzymes for serine synthesis can be epigenetically activated by the histone H3 methyltransferase G9A, to support the survival and proliferation of cancer cells [20]. Folic acid metabolic disorders caused by diet or genetic reasons are sustained by the metabolism of one-carbon units and violate processes of synthesis and methylation of DNA [10, 16, 18, 21]. Moreover, the high level of polyamine biosynthesis in cancer cells makes them vastly dependent on metabolism of the folates and one-carbon units.

Recently, particular attention has been devoted to the study of cellular regulatory systems. They are investigated by means of metabolic modeling, which is a promising approach for in silico prediction of cell activity, based on relations and interaction of all cellular components. Computational modeling plays an important role in understanding the mechanisms of metabolic flux redistribution in cancer cells. Mathematical approaches such as flux balance analysis (FBA) are widely used to predict the distribution of metabolic fluxes in various cell types, ranging from bacteria to human cells [22–25]. FBA relies on a stoichiometric model of metabolic network—a set of restrictions on exchange fluxes and objective function (e.g., the maximum level of ATP production), which help to predict intracellular fluxes by the use of linear programming. Although FBA is applied successfully to unicellular organisms as objects of biotechnology and metabolic engineering, its use for the study of metabolic fluxes in human cells is more challenging, due to the difficulty of accurately describing the ways in which cells exchange metabolites with their environment.

We used the flux balance analysis method to develop a mathematical model of folate and methionine-dependent metabolism of polyamines that will enable us to study the properties of cancer cells. The novelty of this paper is in extending the study of interactions in a complex biochemical system using the concept of control-effective flux (CEF) by simulating both overexpression and inhibition of particular enzymes.

Aims of this study were: (i) to develop model that can be used for predicting the behavior of cancer cells of different types; (ii) to determine the metabolic pathways required to maintain the cancer phenotype during changing SAMdc activity; (iii) to find the pathways and targets that could be used by the transformed cell for metabolism reprogramming and surviving during the therapy.

Materials and Methods

The developed stoichiometric model includes the following metabolic pathways: polyamine, methionine, methionine salvage, folate metabolism, and glutathione and taurine synthesis cycles, in addition to uric acid cycle input. The model consists of 51 reactions and 57 metabolites, 31 of which are internal metabolites. The metabolism scheme, which is the basis of the model, is shown in Fig. 1. The full list of model reactions is given in Table 1, Appendix.

The processes of folate, methionine, and glutathione metabolism are built according to [26]. The polyamine cycle is based on studies [4–7, 27]. The description of methionine salvage cycle was taken from [11, 13, 28].

The stoichiometric model was developed using the *CellNetAnalyser 2017.1* software [29] using the comprehensive knowledge of metabolites and binding reactions that occur in the metabolic network.

We used FBA for the mathematical description and analysis of metabolic fluxes. The calculation of the elementary flux modes (EFMs) based on the stoichiometry matrix was used for analysis of important pathways in metabolic networks and identifying the links between metabolic cycles. EFM is defined as a directed path that includes a minimal and unique set of reactions from one external metabolite to another [30]. EFMs were calculated using *CellNetAnalyser 2017.1* and *Metatool 4.3* software [31].

The importance of each reaction for the efficient and flexible operation of the entire metabolic system was assessed using control-effective flux methodics. CEF was determined directly from the EFM set [22]. Efficiency

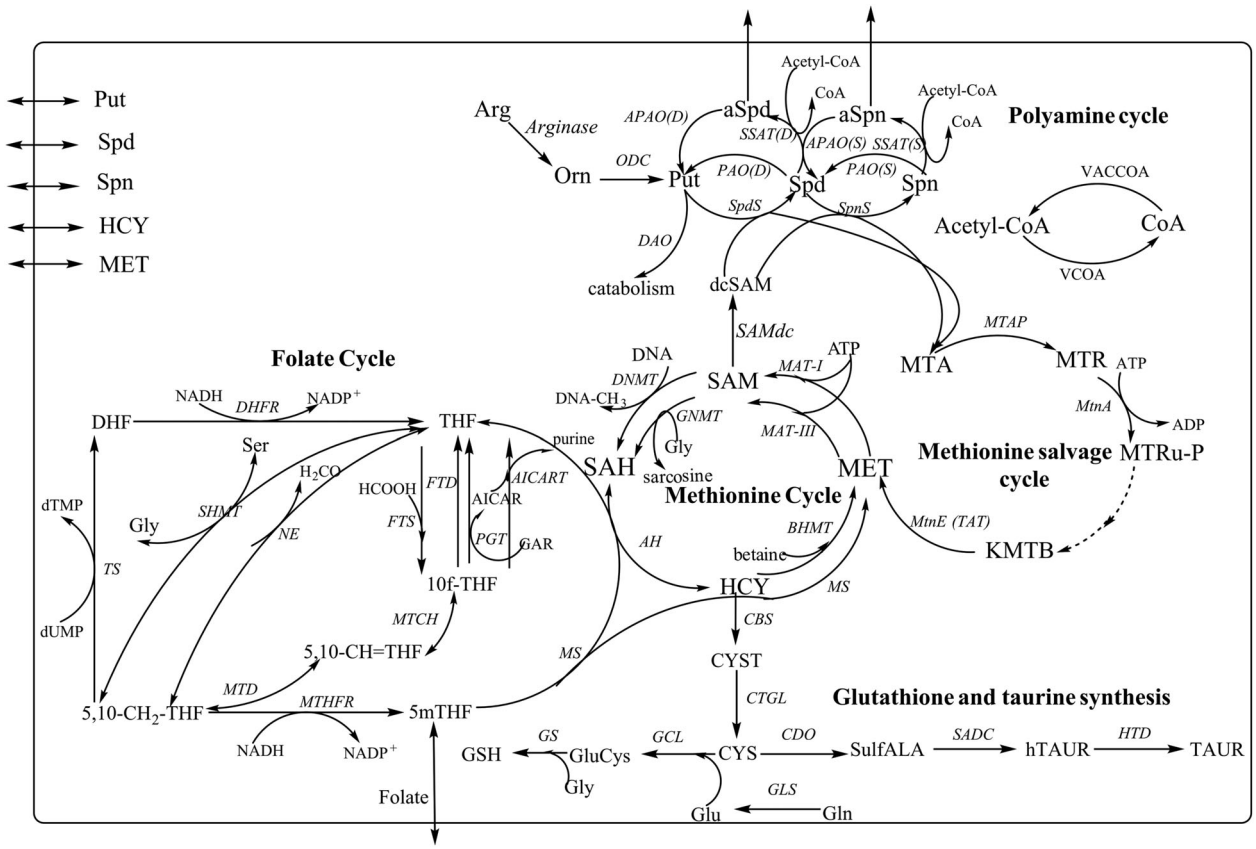

Fig. 1 Metabolic scheme of stoichiometric model. The enzymes are: AH SAH-hydrolase, AICART aminoimidazolecarboxamide ribonucleotide transferase (phosphoribosylaminoimidazolecarboxamide formyltransferase), APAO acetylpolyamine oxidase, BHMT betaine-homocysteine methyltransferase, CBS cystathionine β-synthase, CDO cysteine dioxygenase, CTGL cystathionine γ-lyase, DAO diamine oxidase, DHFR dihydrofolate reductase, DNMT DNA-methyltransferase, FTD 10-formyltetrahydrofolate dehydrogenase, FTS 10-formyltetrahydrofolate synthase, GCL glutamate-cysteine ligase (γ-glutamylcysteine synthetase), GLS glutaminase, GNMT glycine N-methyltransferase, GS glutathione synthetase, HTD hypotaurine dehydrogenase, MAT methionine adenosyltransferase, MS methionine synthase, MTAP methylthioadenosine phosphorylase, MTCH 5,10-methenyltetrahydrofolate cyclohydrolase, MTD 5,10-methylenetetrahydrofolate dehydrogenase, MTHFR 5,10-methylenetetrahydrofolate reductase, MtnA methylthioribose-1-phosphate isomerase, MtnE (TAT) tyrosine aminotransferase, NE nonenzymatic interconversion of THF and 5,10-CH_2-THF, ODC ornithine decarboxylase, PAO polyamine oxidase, PGT phosphoribosyl glycinamide-transformalase, SADC cysteine sulphinic acid decarboxylase, SAHH S-adenosylhomocysteine hydrolase, SAMdc S-adenosylmethionine decarboxylase, SHMT serinehydroxymethyl transferase, SpdS spermidine synthase, SpmS spermine synthase, SSAT spermidine/spermine acetyltransferase, TS thymidylate synthase, VACCOA acetyl–CoA synthetase, VCOA N-acetyltransferase. The metabolites are: 10f-THF 10-formyltetrahydrofolate, 5mTHF 5-methyltetrahydrofolate, 5,10-CH=THF 5,10-methenyltetrahydrofolate, 5,10-CH_2-THF 5,10-methylenetetrahydrofolate, AICAR aminoamidazolecarboxamide ribotide, Arg arginine, aSpd N-acetylspermidine, aSpn N-acetylspermine, CYS cysteine, CYST cystathionine, dcSAM decarboxylated S-adenosylmethionine, DHF dihydrofolate, dTMP deoxythymidine monophosphate, dUMP deoxyuridine monophosphate, GAR glycinamide ribonucleotide, Gln L-glutamine, Glu L-glutamate, GluCys glutamyl-cysteine, GSH glutathione, Gly glycine, HCY homocysteine, hTAUR hypotaurine, KMTB 2-keto-4-methylthiobutyrate, MET methionine, MTA S-methyl-5-thioadenosine, MTR S-methyl-5-thioribose, MTRu-P S-methyl-5-thioribulose-1-phosphate, Orn ornithine, Put putrescine, SAH S-adenosyl-L-homocysteine, SAM S-adenosylmethionine, Ser serine, Spd spermidine, Spn spermine, SulfALA 3-sulfinoalanine, TAUR taurine, THF tetrahydrofolate

values for cellular objective reactions of each elementary flux mode were calculated using the following equation:

$$\varepsilon_{j,\,CELLOBJ} = \frac{r^{j}_{CELLOBJ}}{\sum_i \left| r^{j}_{i} \right|},$$

where $r^{j}_{CELLOBJ}$ is the yield of production of the cellular objective by EFM (reactions related to cellular objectives), and $\sum_i \left| r^{j}_{i} \right|$ is the sum of the participation coefficients of each reaction in a certain EFM (the sum of absolute fluxes of each mode), "*j*" is the EFM index, "*i*" is the flux index through over a specific reaction in certain EFM [22, 24]. To calculate $\varepsilon_{j,CELLOBJ}$, we used r^{j}_{i} for the fluxes of reactions catalyzed by the enzymes MAT-I, DNMT, MS, SSAT (D), SSAT (S), VACCOA, MTHFR, SHMT, GS, GLS (to decipher acronyms see legend to Fig. 1). These reactions

have a significant effect on the cell condition, especially on the processes of cellular tumor metabolism reprogramming.

The CEF (υ_i) of each reaction (r_i^j) was defined as the mean flux through this reaction in all EFMs, where the flux through each mode is weighted with its efficiency [22]:

$$\upsilon_i = \sum_{CELLOBJ} \frac{1}{r^{max}_{CELLOBJ}} \frac{\sum_j \varepsilon_{j,CELLOBJ} \left| r_i^j \right|}{\sum_j \varepsilon_{j,CELLOBJ}}$$

where $r^{max}_{CELLOBJ}$ is the maximum participation rate in the EFM for reactions that are the part of the cellular objective, $\sum_j \varepsilon_{j,CELLOBJ} \left| r_i^j \right|$ is the sum of the products of the participation coefficients of each reaction for all EFMs and the corresponding efficiency values, $\sum_j \varepsilon_{j,CELLOBJ}$ is the total value of the efficiency of the reactions of cellular objective for each mode.

To determine the behavior of the entire metabolic system under the condition of a particular enzyme's deficiency, the coefficients of the reaction participation r_i^j in the EFM that include the deficient enzyme were multiplied by the constant d_j to reflect the level of enzyme inactivation, with values from 1 to 0, where 1 is complete inactivation of the enzyme. To evaluate the behavior of the metabolic network by the enzyme activation the coefficients were multiplied by the constant m_j, which represents the degree of the enzyme activation and takes values from 1 to 4.

Results

Elementary Flux Modes Analysis of Polyamine Metabolism

A total of 292 elementary fluxes have been calculated for the developed model of metabolism of polyamines; 35 of which were extreme paths. Thus, there are 257 pathways to describe all possible ways of distributing stationary fluxes. Fluxes were divided into five groups depending on the involved metabolic cycles and final metabolites. 84 elementary fluxes pass through the folate and methionine cycles, 48 of which involve the initial and final metabolites of these metabolic cycles, and 36 of them involve the external metabolites from the methionine and folate cycles and move to the glutathione cycle. The final products in this case are glutathione and taurine.

Polyamines and their acetylated derivatives are synthesized in 173 metabolic fluxes. In 13 of them polyamines are formed from arginine, from polyamines entering the cell from outside, and from their acetylated forms in catabolism. These processes take place without complete inactivation of SAMdc via inhibitors leads to a decrease in the concentration of spermine (Spn) and spermidine (Spd); however, when compared, the concentration of putrescine (Put) is higher [32]. Put is formed in the fluxes that remain after SAMdc inactivation, and the products of polyamine catabolism accumulate due to the entry of Spn and Spd from outside of the cell.

In 160 elementary fluxes, the production of polyamines and other metabolites involves folate, methionine, and polyamine cycles. All 160 elementary flux modes, in which polyamines are synthesized include the methionine salvage cycle, indicating its importance for regulating the total pool of polyamines, methionine, and other vital cell metabolites. Various mechanisms of catabolism of polyamines are realized in 44 elementary fluxes. Thus, we can see that the catabolism of polyamines is equally important for the regulation of the content of polyamines.

Complete inactivation of SAMdc will block 160 elementary fluxes in the metabolic network of the cell.

CEF Analysis of the Metabolic Network

The CEF numeric values for a case that SAMdc is a normally functioning enzyme are shown in Table 1 (see Appendix). We can see that the peak CEF indicators are characteristic for folate cycle enzymes that mostly indicates the importance of the metabolites formed in this cycle for the functioning of the methionine cycle and the production of SAM and polyamines. Enzymes of polyamine metabolism exhibit significantly lower CEF values, even in comparison with the methionine cycle and the methionine salvage cycle. The least CEF coefficients (CEFs) have enzymes of the folate cycle phosphoribosyl glycinamidetransformalase (PGT) and phosphoribosylaminoimidazolecarboxamide formyltransferase (AICART), which control the synthesis of purine nucleotides.

Figures 2–4 show changes in CEFs of reactions depending on the degree of activation (inactivation) of SAMdc. CEFs are normalized with respect to the indicator value for a normally functioning enzyme. On the abscissa axis to the right: 0—normally functioning enzyme, 1—complete enzyme inactivation. The enzyme activity increases from zero to the left (up to 4 times).

According to the simulation results, the growth of SAMdc activity leads to an increase in fluxes through the enzymes of polyamine synthesis. However, this growth is insignificant and does not exceed 10% (Fig. 2). The tumor growth is accompanied by inhibition of catabolic processes, including the activity of spermine/spermidine acetyltransferases [33]. The simulation results show that fluxes through SSAT are reduced by 20–30% from the initial level when SAMdc is activated. At the same time, the catabolism of polyamines significantly slows down (Fig. 2). Increasing the activity of SAMdc by a factor of 4 leads to a decrease of the Put catabolism by more than 70%, to a reduction in fluxes through polyaminoxidases (PAO(S), PAO(D)) and acetylpolyamineoxidases (APAO(S), APAO(D)) by more

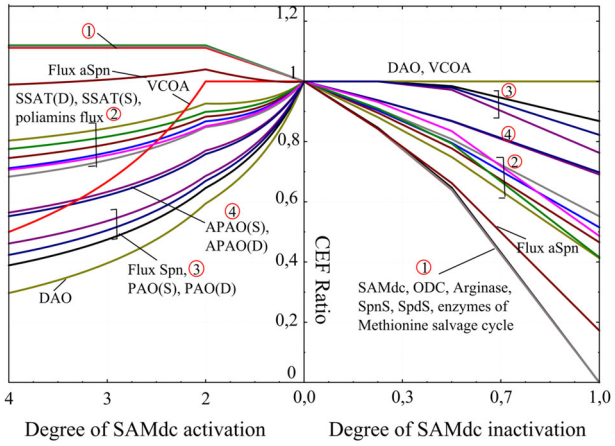

Fig. 2 Changes in polyamine cycle CEFs upon the change of SAMdc activity. In this and the following figures *y*-axis indicates CEF ratios with respect to the normal case. In *x*-axis, 0 shows fully functional enzyme, 1 (right) depicts a complete deficiency of the enzyme, the scale on the left indicates an increase in enzyme activity from two to four times

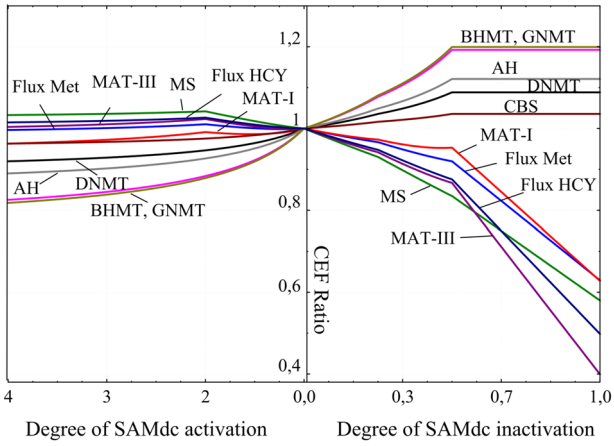

Fig. 3 Changes in methionine cycle CEFs upon the change of SAMdc activity

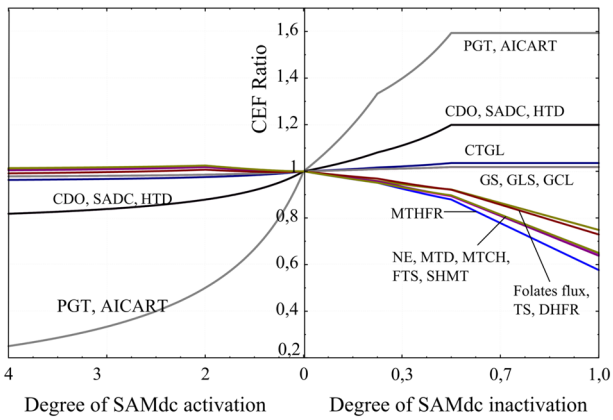

Fig. 4 Changes in folate cycle, glutathione and taurine synthesis pathway CEFs upon the change of SAMdc activity

than a half. Therefore, it can be argued that the increase in the activity of SAMdc causes the increase in the content of polyamines, and that is not due to their synthesis, but because of reducing their catabolism and the processes of acetylation.

The increased activity of SAMdc leads to a decrease in fluxes through the enzymes of the methionine cycle, but no more than by 20% (Fig. 3). Thus, fluxes through MS, MAT-III, and fluxes of external metabolites (such as methionine and homocysteine), slightly exceed the control level. These fluxes support the formation of SAM.

Simulation indicates a slight increase in flux through methyltetrahydrofolate reductase (MTHFR) when SAMdc is activated (Fig. 4). It contributes to an increase in the flux of one-carbon units to the methionine cycle and to the maintenance of the SAM biosynthesis through the synthesis of deoxythymidine monophosphate (dTMP). The most susceptible to the activation of SAMdc are the enzymes that involve cysteine to the process of taurine synthesis (decrease in activity down to 20% from norm), AICART and PGT, which are implicated in de novo synthesis of purines. For these reactions, CEFs are reduced by more than 60% with a four times increase in SAMdc activity (Fig. 4). These results allow us to make predictions for changes in metabolic processes when increasing the activity of this enzyme.

As we can see from the results of simulation, when SAMds is inactivated by more than 50%, the fluxes through all the enzymes of polyamine catabolism decrease, but the decline does not exceed 20% (Fig. 2). Fluxes through the reactions of catabolism of Put, Spn, and Spd will not change within the 50% SAMdc inactivation level, but will decrease if the activity of the enzyme is less than 50%. SAMdc inactivation will reduce the fluxes through the enzymes of Spn and Spd synthesis and acetylation. Therefore, the reduction of the activity of SAMdc to more than 50% of the norm leads to a decrease in the total pool of polyamines by inhibiting their synthesis and the constant rate of catabolism.

The complete inactivation of SAMdc will result in total inhibition of fluxes through ODC, arginase, and methionine salvage cycle. Enzymes that operate consistently with SAMdc are enzymes of the methionine salvage cycle—spermine/spermidine synthases (SpnS and SpdS). In this regard, the effects of the activation/inactivation of these enzymes on the redistribution of fluxes in the metabolic network will be similar to SAMdc.

The simulation results indicate that the inactivation of SAMdc causes significant changes in metabolic pathways through the methionine cycle (Fig. 3). CEF analysis showed that inactivation of SAMdc down to 50% results in an increase of fluxes through glycine N-methyltransferase

(GNMT) by 20% and through DNA-methyltransferase (DNMT) by 10%. Subsequent inactivation of SAMdc does not increase the fluxes of methylation; they remain at the same level. DNMT is an enzyme that belongs to DNA-methyltransferases that control the process of DNA methylation. Therefore, normal activity of the enzymes of this class is integral to a normal cell life span.

With inactivation by more than 50% we observed a decrease in the flux through the enzymes MAT-I and MAT-III that directly affect the formation of SAM from methionine. Complete inactivation of SAMdc leads to stopping the flux through MAT-III, and the flux through MAT-I is decreased by 40%. Thus, the decrease in SAM synthesis concurrent with its increased demand in the methylation processes will lead to a reduction of the SAM/SAH ratio.

Another outcome of SAMdc activity decrease is significant inactivation of MS. Re-methylation of homocysteine in the MS reaction has a critical role for folic acid metabolism. It singularly regulates the return of 5mTHF to a pool of active folates involved in the synthesis of purines, thymidylate, and provides the ability to regenerate methionine in all organs and tissues of mammals. The decrease in the flux through MS causes the drop in flux through MTHFR (Fig. 4). CEF for this enzyme is reduced by more than 40% when SAMdc is completely inactivated.

The study of flux redistribution with inactivation of SAMdc show that under conditions of MS inactivation, the HCY remethylation takes place due to betaine-homocysteine methyltransferase (BHMT). CEF for this enzyme increases by 20% when SAMdc is inactivated by more than 50%. The deficiency of MS results in the accumulation of 5mTHF due to THF and methylenetetrahydrofolate that in turn leads to the termination of de novo synthesis of thymidylate [34]. Accordingly, the decrease in thymidylate synthase (TS) expression is detected, which results in the accumulation of dUMP and reduce the consumption of 5,10-methylene-THF, which is a substrate for both TS and MTHFR. These processes occur in tumors that are folate-depleted [10].

According to the simulation results, the fluxes through GAR and AICAR, important enzymes for the de novo purine nucleotides synthesis, are significantly increased (Fig. 4).

Reducing the fluxes through MS and MTHFR and enhancing the trans-methylation processes results in an increase in the HCY concentration, which then increases activity through cystathionine β-synthase (CBS), the first enzyme in the trans-sulfation pathway. According to the simulation, inactivation of SAMdc increases the flux through CBS (Fig. 3) and amplifies the production of glutathione and taurine (see Fig. 1). At the stage of cysteine formation, where the pathway branches out, the flux shifts towards the formation of taurine. According to the simulation, the rate of the flux through cysteine dioxygenase (CDO) exceeds fluxes through CBS and cystathionine γ-lyase (CTGL). CDO catalyzes the oxidation of cysteine to sulfinoalanine and represents the first step in the pathways leading to the synthesis of sulfate/pyruvate or hypotaurine/taurine.

Such activities of key enzymes in cysteine catabolism (cysteine dioxygenase and γ-glutamylcysteine synthetase) occurs in conditions of protein deficiency. That is associated with the accelerated utilization of cysteine excess and the accumulation of homocysteine with the progress of hyperhomocysteinemia [35].

Discussion

The development of biochemical and molecular-biological methods for the study of the tumor cell metabolism contributed to furthering our understanding of the mechanisms and effects of tumor-associated metabolic disorders at various stages of tumor formation. Subsequent research has attempted to understand the underlying mechanisms for the metabolic profile change, which meet the metabolic demand during carcinogenesis. To address these questions, it is critical to combine the use of high-performance experimental and computational models that can determine which metabolic pathways are necessary to support the cancerous phenotype and how these pathways are organized to support vital processes in the proliferation of cancer cells. Understanding this phenomenon is crucial for the development of systematic schemes that help to identify the mechanisms that promote or delay the malignancy development.

We present and discuss the computational analysis of methionine-dependent metabolic pathways in cancer cells. One should remember that metabolic features are heterogeneous, and each cancerous cell has peculiar metabolic features, depending on its genetic, epigenetic, and environmental status. At this stage, our model does not take into account all the diversity of enzymatic expression in specific cancer cells. Nevertheless, the developed model can be easily adapted to a specific type of metabolism and expression to calculate the metabolic fluxes in definite cell types.

There are several models based on FBA. This method uses stoichiometry data and information about the reversibility or irreversibility of reactions—it does not require complex mathematical computations and can be easily implemented as software for computing experiments. This approach allows to estimate the distribution of metabolic fluxes (or steady velocities) and their relative contribution to the formation of particular metabolite. Analysis of fluxes in a metabolic network consisting of cellular reactions allows to establish a relation between the genotype and the

phenotype of cell [23]. There are some limitations to FBA, which primarily include restriction by a steady state of flux and the inability to trace allosteric effects from the metabolites.

One of the main approaches to the analysis of metabolic network fluxes is the metabolic pathway analysis (MPA) [36], which is used to determine the structure of the metabolic network and the general possibilities of cell metabolism. An important tool used in MPA is the identification of EFMs – a minimal set of enzymes that can operate in a steady-state weighted by the input fluxes [22, 24, 37]. EFM analysis allows us to detect and analyze important pathways in metabolic networks. Another tool for metabolism assessment is the CEF analysis [22, 24, 38]. CEF value derived directly from the EFM set, represents the importance of each metabolic reaction for the efficient and flexible operation of the entire metabolic network.

The difficulty of using the tool of control-effective flux (CEF) for complex cell types is in the choice of reactions that should be taken into account in the cellular objective. The choice of a cellular objective affects the values of control-effective flux, since the efficiency of each EFM is evaluated by determining its contribution towards definite cell objective relative to the costs needed to establish the mode of cell functioning [38]. A significant advantage of this approach is taking into account not only the optimal route, but also the complete set of possible pathways, which leads to redundancy and flexibility in the metabolic network. In addition, this approach does not require defining the limits of exchange fluxes [24].

We used stoichiometric modeling to investigate the effects of SAMdc inactivation, since this enzyme is a common antitumor therapy target. Cancer cells require high level of polyamines and up to 70% of cell SAM provides this biosynthesis [39]. The simulation showed that the increase in the expression of SAMdc indeed increases the level of polyamines, as simultaneously the fluxes through SpmS, SpdS, ODC, and arginase increase. But fluxes through the pathways of polyamine catabolism decrease. This result shows pretty good congruence with the experimental data indicating a significant inhibition of the polyamine catabolism under conditions of SAMdc activity intensification observed in tumor growth [6, 40]. However, the model does not predict a significant increase in the level of polyamines that coincides with topical studies on overexpression of SAMdc and SpmS in transgenic mice, which showed that more than 100 times increase in expression of SAMdc and more than 9 times increase in expression of SpmS and SpdS does not lead to a significant increase in the level of polyamines in tissues [41, 42].

Methionine helps to meet the increased demand for SAM. The calculations predict a slight increase in the fluxes through MS, MAT-I/MAT-III, and a notable increase in flux through the methionine salvage cycle. S-methyl-5-thioadenosine phosphorylase (MTAP) plays a main role in the methionine salvage processes, because this enzyme provides transformation of significant amount of S-methyl-5-thioadenosine (MTA, the product of SAM decarboxylation) to methionine. However, the activity of MTAP differs depending on specific forms of cancer. For example, the MTAP gene is excreted in many cancer cell lines [43], but in those that retain the expression of MTAP, like in prostate cancer, high levels of SAM and polyamines were recorded [11]. The model predicts a significant reduction in the fluxes through the enzymes of purine synthesis and a slight decrease in the fluxes through the cycle of trans-sulfation. MTAP is a unique enzyme that provides rapid processing of MTA to adenine. Subsequent transformation of adenine into AMP depends on the activity of adenine phosphoribosyl transferase (APRT) in purine salvage pathway. Therefore, we can conclude that fluxes through APRT and AICART are less important when MTAP is activated.

According to the simulation results, the increase in concentration of SAM will not significantly affect the processes of DNA methylation and the functioning of most enzymes of the folate cycle. Maintaining the high level of polyamines is also possible by the activation of the methionine cycle where SAM consumption is accompanied with the removal of the methyl group [10]. One way to balance the flux is to receive a carbon unit from the folate cycle through MTHFR to the methionine cycle. Although experimental study did not detect significant increase in the expression of MTHFR [10], SAM is an allosteric inhibitor of MTHFR activity, and therefore increasing the consumption of SAM by increasing the expression of SAMdc will increase the activity of MTHFR and the flux of one-carbon units.

Our model points to several curious implications of SAMdc inhibitors that potentially could enhance the efficacy of chemotherapy.

Our study showed that SAMdc inactivation leads to the decrease in fluxes through MS, MAT-I/MAT-III, and folate cycle. According to the literature, such processes occur in methionine-dependent tumors, including prostate cancer, lung cancer, fibrosarcoma, melanoma [21], breast cancer [44]. In listed above tumor cells, that are sensitive to L-methionine deficiency, the reduced level of MS and MTAP expression [45], as well as disrupted folate metabolism is observed. The methionine dependence was also found in the primary culture of tumors taken from patients [46, 47].

However, we show that, despite the reduction of methionine synthesis and salvage, it remains possible to synthesize methionine from homocysteine and betaine, as evidenced by a significant increase in flux through SAH-hydrolase (AH) and BHMT. But most cancer cells cannot proliferate when methionine is replaced with homocysteine, while non-cancer

cells are indifferent to such replacement. The inability of tumor cells to maintain a sufficient level of methylation in a methionine-free homocysteine-enriched medium proves the need for exogenous methionine [45]. It indicates that methionine and folate restriction may inhibit cancer cell growth and may enhance the efficacy of chemotherapeutic agents. Two reviews analyze the results of studies that indicate the prospects of dietary restriction of methionine [21, 46]. So, dietary folate manipulations in models of transgenic adenocarcinoma of the prostate (TRAMP) [10, 18] and breast cancer [48] revealed that folate restriction significantly reduces disease progression with reductions in tumor grade, lymph node metastasis, decreased recurrence rate. The threat is the tumors may reprogram and continue further growth under certain conditions, e.g., a diet enriched with folates and methionine [2, 10].

Along with SAMdc inactivation driven reduction of the methionine pool and the adenosine trans-methylation processes, the increased DNA and glycine methylation in a GNMT-catalyzed reaction was detected in our model. GNMT, as methyltransferase, catalyzes the transfer of the methyl group from SAM to glycine to form S-adenosylhomocysteine (SAH) and sarcosine (N-methylglycine). This enzyme is not expressed in most cancer cells [39] that presumably helps to maintain high level of SAM and polyamines. However, GNMT is reported to be expressed in prostate carcinoma [49, 50] and breast cancer [51]. It leads to a decrease in SAM/SAH ratio in these cells and to the accumulation of sarcosine. Sarcosine has mostly been researched in prostate cancer [52]. Studies have shown that increased sarcosine levels are associated with cancer progression and metastasis. Sarcosine stimulates the expression of DNA methyltransferase (DNMT), DNA hypermethylation, resulting in epigenetic changes in cancer. These studies could be considered in chemotherapy with SAMdc inhibitors for tumors with high GNMT expression, that could be complemented with GNMT or DNMT inhibitors.

The important result of our simulation is that inactivation of SAMdc leads to a significant increase in the fluxes through GAR and AICAR, involved in de novo synthesis of purine nucleotides with serine participation. These enzymes, together with the cytoplasmic and mitochondrial serine hydroxymethyltransferase (SHMT), are already known targets for antitumor therapy, as they are involved in metabolic reprogramming that support tumor progression [3, 53]. Serine may supply one-carbon units for homocysteine to methionine conversion and thus maintain methionine cycle in case of methionine depletion. Maddocks et al. [14] found that serine supports DNA methylation by de novo ATP synthesis. They showed that serine starvation significantly decreases transfer of methyl groups from methionine to DNA compared to a serine-supplemented culture and decreases the level of ATP, SAM, and S-adenosylhomocysteine (SAH) [17]. Serine-dependent de novo ATP synthesis is necessary to support the transformation of methionine to SAM, and the restriction of this ATP pool can affect SAM generation rate, as well as methylation of DNA and RNA [14]. Thereby, due to the increased uptake of exogenous serine in tumors, dietary restrictions on serine and glycine are recommended [15]. In addition, serine can be formed in the glycolytic pathway [48]. Increased expression of 3-phosphoglycerate dehydrogenase (PHGDH), a rate-limiting serine biosynthesis enzyme, is shown in breast cancer and melanoma [3]. Therefore, restriction of glucose intake potentially could be helpful [8].

In silico simulation also indicates that during SAMdc inactivation homocysteine is involved in the transsulfuration pathway, which is known to be reprogrammed in cancer. Indeed, experiments in homocysteine-labeled breast cancer cells MDA-MB468 have revealed a deviation of the flux from the methionine cycle to the transsulfuration pathway [44]. The same experiments indicated the reduced SAM synthesis, resulting in a reduced overall methylation potential, and, therefore, the reduced SAM/SAH ratio. Some authors [21] suggest that low SAM or SAM/SAH ratios are key points to understanding the Hoffmann effect, and that increased flux through the transsulfuration pathway may induce these changes in the methylation potential. Such a redirection of homocysteine to the transsulfuration branch is induced by oncogenic mutations in phosphoinositide 3-kinase (PI3K), which result in a methionine-dependent phenotype [54]. Cysteine, the first metabolite of transsulfuration pathway, in rapidly proliferating cells can be involved in the biosynthesis of glutathione and iron-sulfur clusters, as well as hydrogen sulfide (H_2S). We show the activation of the H_2S formation pathway. It is believed to be involved in protection against oxidative stress, excessive mitochondrial respiration, it blocks apoptosis and promotes angiogenesis [3].

Therefore, when using therapeutic agents aimed at SAMdc inactivation, the possibility of reprogramming of tumor cellular metabolism should be considered, as well as the use of SAM in methylation and catabolism of serine. Understanding the metabolic changes that distinguish cancer cells from normal ones requires a systems approach, that allows the identification of mechanisms that support the cancer phenotype, and this understanding will contribute to the development of personalized and thus, more effective treatment. FBA can be a useful tool for this goal.

Conclusions

The developed stoichiometric mathematical model of polyamine metabolism includes polyamine, folate, methionine, glutathione cycles, and methionine salvage cycle. The model also includes inputs from cycles of uric acid and the incomes

of metabolites from outside of the cell. We used the calculations of the number of elementary modes and the coefficients of control-effective flux to analyze the behavior of polyamine metabolic network. The model extended the possibilities for analyzing interactions in a complex biochemical system using CEF to simulate the behavior of the network by overexpression and inhibition of a specific enzyme.

We have performed in silico analysis of the behavior of the methionine-dependent metabolic network of polyamines at the activation of SAMdc, which is usually observed in tumor development. The simulation results are clearly congruent with previous experimental studies. That indicates the possibility of using this model to predict cellular processes or formulate certain hypotheses.

We have shown that the activity of SAMdc has a strong impact on the fluxes in methionine and folate cycles. It affects these fluxes significantly more than the polyamine cycle. Inactivation of SAMdc leads to momentous redistribution of fluxes through the methionine cycle, namely, the enhancement of methylation processes, the transformation of SAM to homocysteine, and the intensification of transsulfuration processes that activate glutathione and taurine synthesis pathway. Cells become methionine depleted. Reducing the synthesis of SAM and its intensified use in the methylation processes create conditions for decreasing the SAM/SAH ratio, which is typical for cancer cells. It is also significant that SAM affects serine methylation and activates serine-dependent de novo ATP synthesis. Lack of methionine may cause additional metabolic alterations in methionine-dependent tumors. Therefore, the possibility of reprogramming of tumor cellular metabolism and the use of SAM in processes of serine methylation and serine catabolism must be closely considered when using therapeutic agents aimed at SAMdc inactivation.

Acknowledgements We outspeak our deep appreciation to the reviewers for their professional remarks. We express our sincere gratitude to Myroslava Tsukanova, Audrey Abend, and Irena Pavliuk for their meaningful advice and valuable language help. Great thanks to Artem Mishchenko for the help with artwork preparation.

Compliance with Ethical Standards

Conflict of Interest The authors declare that they have no conflict of interest.

Appendix

Table 1 Reactions included to the model, enzymes and their CEF values (arrow type → or ↔ indicates whether the reaction is considered irreversible or reversible in the analysis)

No	Reactions	Enzymes	CEF
Methionine cycle reactions			
1	Met + ATP → SAM + ADP	MAT-I	2,79
2	Met + ATP → SAM + ADP	MAT-III	2,21
3	SAM + Gly → SAH	GNMT	0,85
4	SAM + DNA → SAH + DNA-CH_3	DNMT	1,85
5	SAH ↔ Hcy + adenosine	AH	2,70
6	Hcy + 5mTHF → MET + THF	MS	2,59
7	Hcy + betaine → MET	BHMT	0,33
Polyamine cycle reactions			
Polyamine synthesis			
8	SAM + H^+ → dcSAM + CO_2	SAMdc	2,29
9	dcSAM + Spd → Spn + MTA	SpnS	1,03
10	dcSAM + Put → Spd + MTA	SpdS	1,26
11	Arg → Orn	Arginase	0,48
12	Orn + H^+ → Put + CO_2	ODC	0,48
13	Spd + Acetyl-CoA → aSpd + CoA	SSAT(D)	1,56
14	Spn + Acetyl-CoA → aSpn + CoA	SSAT(S)	1,56
Polyamine catabolism			
15	aSpd + O_2 + H_2O → Put + H_2O_2 + 3-AAP	APAO(D)	0,78
16	aSpn + O_2 + H_2O → Spd + H_2O_2 + 3-AAP	APAO(S)	0,87
17	Put + O_2 + H_2O → 4-aminobutanal + NH_3 + H_2O_2	DAO	0,35
18	Spd + O_2 + H_2O → H_2O_2 + 4-aminobutanal	PAO(D)	0,21
19	Spn + O_2 + H_2O → H_2O_2 + 3-aminopropanal	PAO(S)	0,28
20	CoA → Acetyl-CoA	VACCOA	3,17
21	Acetyl-CoA → CoA	VCOA	0,04
Fluxes			
22	aSpd → out of the cell	Flux acetylspermidine	0,78
23	aSpn → out of the cell	Flux acetylspermine	0,69
24	Put_out ↔ Put_in	Flux putrescine	0,84
25	Spd_out ↔ Spd_in	Flux spermidine	0,77
26	Spn_out ↔ Spn_in	Flux spermine	1,1
27	MET_out ↔ MET_in	Flux methionine	4,17
28	Hcy_out ↔ Hcy_in	Flux homocysteine	3,21
29	5mTHF_out ↔ 5mTHF_in	Flux 5mTHF	4,87
Methionine salvage cycle reactions			
30	MTA + H_2O → MTR + adenine	MTAP	2,29
31	MTR → MTRu-P	MtnA	2,29
32	MTRu-P → KMTB (*includes several sequential stages*)		2,29

Table 1 (continued)

No	Reactions	Enzymes	CEF
33	KMTB + $C_5H_9NO_4$ → MET + $C_5H_6O_5$	MtnE (TAT)	2,29
Folate cycle reactions			
34	5,10-CH2-THF + NADPH + H^+ → 5mTHF + $NADP^+$	MTHFR	7,10
35	5,10-CH=THF + NADPH + H^+ ↔ 5,10-CH_2-THF + $NADP^+$	MTD	11,64
36	10f-THF ↔ 5,10-CH=THF + H_2O	MTCH	11,64
37	ATP + $HCOO^-$ + THF ↔ ADP + Pi + 10f-THF	FTS	11,59
38	10f-THF + GAR → THF + AICAR	PGT	0,02
39	10f-THF + AICAR → THF + FAICAR	AICART	0,02
40	5,10-CH2-THF + dUMP → DHF + dTMP	TS	4,54
41	DHF + NADPH + H^+ → THF + $NADP^+$	DHFR	4,54
42	THF + Ser ↔ 5,10-CH2-THF + Gly + H_2O	SHMT	11,90
43	5,10-CH2-THF ↔ THF + H_2CO	NE	11,38
Transsulfuration reactions			
44	Hcy + Ser → Cyst + H_2O	CBS	2,38
45	Cyst + H_2O → Cys + NH_3 + akbut	CTGL	2,38
Reactions of glutathione transformation			
46	ATP + Cys + Glu → ADP + GlutCys + Pi	GCL	2,15
47	ATP + GluCys + Gly → ADP + GSH + Pi	GS	2,15
Taurine synthesis reactions			
48	Cys + O_2 → SulfALA	CDO	0,23
49	SulfALA → CO_2 + hTAUR	SADC	0,23
50	hTAUR + H_2O + NAD^+ ↔ TAUR + NADH + H^+	HTD	0,23
Glutamic acid transformation			
51	Gln + H_2O → Glu + NH_3	GLS	2,15

Previously undefined acronyms are: *3-AAP* 3-acetamidopropanal, *akbut* α-ketobutyrate, *FAICAR* 5-formamidoimidazole-4-carboxamide ribotide, *Pi* phosphate

References

1. Soda, K. (2020). Spermine and gene methylation: a mechanism of lifespan extension induced by polyamine-rich diet. *Amino Acids*, *52*(2), 213–224. https://doi.org/10.1007/s00726-019-02733-2.
2. Gao, X., Reid, M. A., Kong, M., & Locasale, J. W. (2017). Metabolic interactions with cancer epigenetics. *Molecular Aspects of Medicine*, *54*, 50–57. https://doi.org/10.1016/j.mam.2016.09.001.
3. Pavlova, N. N., & Thompson, C. B. (2016). The emerging hallmarks of cancer metabolism. *Cell Metabolism*, *23*(1), 27–47. https://doi.org/10.1016/j.cmet.2015.12.006.
4. Sánchez-Jiménez, F., Medina, M. Á., Villalobos-Rueda, L., & Urdiales, J. L. (2019). Polyamines in mammalian pathophysiology. *Cellular and Molecular Life Sciences*, *76*, 3987–4008. https://doi.org/10.1007/s00018-019-03196-0.
5. Bae, D. H., Lane, D. J. R., Jansson, P. J., & Richardson, D. R. (2018). The old and new biochemistry of polyamines. *Biochimica et Biophysica Acta*, *1862*(9), 2053–2068. https://doi.org/10.1016/j.bbagen.2018.06.004.
6. Miller-Fleming, L., Olin-Sandoval, V., Campbell, K., & Ralser, M. (2015). Remaining mysteries of molecular biology: the role of polyamines in the cell. *Journal of Molecular Biology*, *427*(21), 3389–3406. https://doi.org/10.1016/j.jmb.2015.06.020.
7. Battaglia, V., Shields, C. D., Murray-Stewart, T., & Casero, R. A. (2014). Polyamine catabolism in carcinogenesis: potential targets for chemotherapy and chemoprevention. *Amino Acids*, *46*(3), 511–519. https://doi.org/10.1007/s00726-013-1529-6.
8. Ruiz-Pérez, M. V., Medina, M. Á., Urdiales, J. L., Keinänen, T. A., & Sánchez-Jiménez, F. (2015). Polyamine metabolism is sensitive to glycolysis inhibition in human neuroblastoma cells. *Journal of Biological Chemistry*, *290*(10), 6106–6119. https://doi.org/10.1074/jbc.M114.619197.
9. Bistulfi, G., Diegelman, P., Foster, B. A., Kramer, D. L., Porter, C. W., & Smiraglia, D. J. (2009). Polyamine biosynthesis impacts cellular folate requirements necessary to maintain S-adenosylmethionine and nucleotide pools. *FASEB Journal*, *23*(9), 2888–2897. https://doi.org/10.1096/fj.09-130708.
10. Affronti, H. C., Long, M. D., Rosario, S. R., Gillard, B. M., Karasik, E., Boerlin, C. S., Pellerite, A. J., Foster, B. A., Attwood, K., Pili, R., Wilton, J. H., Campbell, M. J., & Smiraglia, D. J. (2017). Dietary folate levels alter the kinetics and molecular mechanism of prostate cancer recurrence in the CWR22 model. *Oncotarget*, *8*(61), 103758–103774. https://doi.org/10.18632/oncotarget.21911.
11. Arruabarrena-Aristorena, A., Zabala-Letona, A., & Carracedo, A. (2018). Oil for the cancer engine: the cross-talk between oncogenic signaling and polyamine metabolism. *Science Advances*, *4*(1), eaar2606. https://doi.org/10.1126/sciadv.aar2606.
12. Zhang, Y., Zheng, Q., Zhou, Y., & Liu, S. (2020). Repurposing clinical drugs as AdoMetDC inhibitors using the SCAR strategy. *Frontiers in Pharmacology*, *11*, 248. https://doi.org/10.3389/fphar.2020.00248.
13. Affronti, H. C., Rowsam, A. M., Pellerite, A. J., Rosario, S. R., Long, M. D., Jacobi, J. J., Bianchi-Smiraglia, A., Boerlin, C. S., Gillard, B. M., Karasik, E., Foster, B. A., Moser, M., Wilton, J. H., Attwood, K., Nikiforov, M. A., Azabdaftari, G., Pili, R., Phillips, J. G., Casero, Jr., R. A., & Smiraglia, D. J. (2020). Pharmacological polyamine catabolism upregulation with methionine salvage pathway inhibition as an effective prostate cancer therapy. *Nature Communications*, *11*(1), 52. https://doi.org/10.1038/s41467-019-13950-4.
14. Maddocks, O. D., Labuschagne, C. F., Adams, P. D., & Vousden, K. H. (2016). Serine metabolism supports the methionine cycle and DNA/RNA methylation through de novo ATP synthesis in cancer cells. *Molecular Cell*, *61*(2), 210–221. https://doi.org/10.1016/j.molcel.2015.12.014.
15. Maddocks, O., Athineos, D., Cheung, E., Lee, P., Zhang, T., van den Broek, N. J. F., Mackay, G. M., Labuschagne, C. F., Gay, D., Kruiswijk, F., Blagih, J., Vincent, D. F., Campbell, K. J., Ceteci, F., Sansom, O. J., Blyth, K., & Vousden, K. H. (2017). Modulating the therapeutic response of tumors to dietary serine and glycine starvation. *Nature*, *544*, 372–376. https://doi.org/10.1038/nature22056.

16. Gao, X., Locasale, J. W., & Reid, M. A. (2019). Serine and Methionine Metabolism: Vulnerabilities in Lethal Prostate Cancer. *Cancer Cell*, *35*(3), 339–341. https://doi.org/10.1016/j.ccell.2019.02.014.
17. Li, A. M., & Ye, J. (2020). Reprogramming of serine, glycine and one-carbon metabolism in cancer. *Biochimica et Biophysica Acta (BBA) – Molecular Basis of Disease*, *1866*(10), 165841. https://doi.org/10.1016/j.bbadis.2020.165841.
18. Bistulfi, G., Foster, B. A., Karasik, E., Gillard, B., Miecznikowski, J., Dhiman, V. K., & Smiraglia, D. J. (2011). Dietary folate deficiency blocks prostate cancer progression in the TRAMP model. *Cancer Prevention Research*, *4*(11), 1825–1834. https://doi.org/10.1158/1940-6207.CAPR-11-0140.
19. Konno, M., Asai, A., Kawamoto, K., Nishida, N., Satoh, T., Doki, Y., Mori, M., & Ishii, H. (2017). The one-carbon metabolism pathway highlights therapeutic targets for gastrointestinal cancer (Review). *International Journal of Oncology*, *50*(4), 1057–1063. https://doi.org/10.3892/ijo.2017.3885.
20. Ding, J., Li, T., Wang, X., Zhao, E., Choi, J. H., Yang, L., Zha, Y., Dong, Z., Huang, S., Asara, J. M., Cui, H., & Ding, H. F. (2013). The histone H3 methyltransferase G9A epigenetically activates the serine-glycine synthesis pathway to sustain cancer cell survival and proliferation. *Cell Metabolism*, *18*(6), 896–907. https://doi.org/10.1016/j.cmet.2013.11.004.
21. Kaiser, P. (2020). Methionine dependence of cancer. *Biomolecules*, *10*(4), 568. https://doi.org/10.3390/biom10040568.
22. Çakır, T., Tacer, C. S., & Ülgen, K. Ö. (2004). Metabolic pathway analysis of enzyme-deficient human red blood cells. *Biosystems*, *78*(1–3), 49–67. https://doi.org/10.1016/j.biosystems.2004.06.004.
23. Çakır, T., Alsan, S., Saybaşılı, H., Akın, A., & Ülgen, K. Ö. (2007). Reconstruction and flux analysis of coupling between metabolic pathways of astrocytes and neurons: application to cerebral hypoxia. *Theoretical Biology and Medical Modelling*, *4*(1), 48. https://doi.org/10.1186/1742-4682-4-48.
24. Schwartz, J. M., Barber, M., & Soons, Z. (2015). Metabolic flux prediction in cancer cells with altered substrate uptake. *Biochemical Society Transactions*, *43*(6), 1177–1181. https://doi.org/10.1042/BST20150149.
25. Geryk, J., Krsička, D., Vlčková, M., Havlovicová, M., Macek, Jr., M., & Kremlíková Pourová, R. (2020). The key role of purine metabolism in the folate-dependent phenotype of autism spectrum disorders: an in silico analysis. *Metabolites*, *10*(5), 184. https://doi.org/10.3390/metabo10050184.
26. Reed, M. C., Thomas, R. L., Pavisic, J., James, S. J., Ulrich, C. M., & Nijhout, H. F. (2008). A mathematical model of glutathione metabolism. *Theoretical Biology and Medical Modelling*, *5*(1), 8. https://doi.org/10.1186/1742-4682-5-8.
27. Rodríguez-Caso, C., Montañez, R., Cascante, M., Sánchez-Jiménez, F., & Medina, M. A. (2006). Mathematical modeling of polyamine metabolism in mammals. *Journal of Biological Chemistry*, *281*(31), 21799–21812. https://doi.org/10.1074/jbc.M602756200.
28. Chu, Y., Lai, H., Pai, L., Huang, Y., Lin, Y., Liang, K., & Yeh, C. (2019). The methionine salvage pathway-involving ADI1 inhibits hepatoma growth by epigenetically altering genes expression via elevating S-adenosylmethionine. *Cell Death & Disease*, *10*(3), 240. https://doi.org/10.1038/s41419-019-1486-4.
29. von Kamp, A., Thiele, S., Hadicke, O., & Klamt, S. (2017). Use of CellNetAnalyzer in biotechnology and metabolic engineering. *Journal of Biotechnology*, *261*, 221–228. https://doi.org/10.1016/j.jbiotec.2017.05.001.
30. Gagneur, J., & Klamt, S. (2004). Computation of elementary modes: a unifying framework and the new binary approach. *BMC Bioinformatics*, *5*(1), 175. https://doi.org/10.1186/1471-2105-5-175.
31. Bedaso, Y., Bergmann, F. T., Choi, K., Medley, K., & Sauro, H. M. (2018). A portable structural analysis library for reaction networks. *Biosystems*, *169*, 20–25. https://doi.org/10.1016/j.biosystems.2018.05.008.
32. Autelli, R., Stjernborg, L., Khomutov, A. R., Khomutov, R. M., & Persson, L. (1991). Regulation of S-adenosylmethionine decarboxylase in L1210 leukemia cells: Studies using an irreversible inhibitor of the enzyme. *European Journal of Biochemistry*, *196*(3), 551–556. https://doi.org/10.1111/j.1432-1033.1991.tb15849.x.
33. Murray-Stewart, T., Applegren, N. B., Devereux, W., Hacker, A., Smith, R., Wang, Y., & Casero, Jr., R. A. (2003). Spermidine/spermine N1-acetyltransferase (SSAT) activity in human small-cell lung carcinoma cells following transfection with a genomic SSAT construct. *Biochemical Journal*, *373*(2), 629–634. https://doi.org/10.1042/bj20021895.
34. Smulders, Y. M., Smith, D. E. C., Kok, R. M., Teerlink, T., Swinkels, D. W., Stehouwer, C. D. A., & Jakobs, C. (2006). Cellular folate vitamer distribution during and after correction of vitamin B12 deficiency: a case for the methylfolate trap. *British Journal of Haematology*, *132*(5), 623–629. https://doi.org/10.1111/j.1365-2141.2005.05913.x.
35. Jiang, H., Hurt, K. J., Breen, K., Stabler, S. P., Allen, R. H., Orlicky, D. J., & Maclean, K. N. (2015). Sex-specific dysregulation of cysteine oxidation and the methionine and folate cycles in female cystathionine gamma-lyase null mice: a serendipitous model of the methylfolate trap. *Biology Open*, *4*(9), 1154–1162. https://doi.org/10.1242/bio.013433.
36. Tröndle, J., Schoppel, K., Bleidt, A., Trachtmann, N., Sprenger, G. A., & Weuster-Botz, D. (2020). Metabolic control analysis of L-tryptophan production with Escherichia coli based on data from short-term perturbation experiments. *Journal of Biotechnology*, *307*, 15–28. https://doi.org/10.1016/j.jbiotec.2019.10.009.
37. Trinh, C. T., & Thompson, R. A. (2012) In: X. Wang, J. Chen, P. Quinn, (eds.). Elementary mode analysis: a useful metabolic pathway analysis tool for reprograming microbial metabolic pathways. *Reprogramming microbial metabolic pathways*. *Subcellular Biochemistry, vol. 64* (pp. 21–42). Dordrecht: Springer.
38. Dotsenko, O. I. (2019). In silico study of peculiarities of metabolism of erythrocytes with glucosephosphate isomerase deficiency. *Regulatory Mechanisms in Biosystems*, *10*(3), 306–313. https://doi.org/10.15421/021947.
39. DebRoy, S., Kramarenko, I. I., Ghose, S., Oleinik, N. V., Krupenko, S. A., & Krupenko, N. I. (2013). A novel tumor suppressor function of glycine N-methyltransferase is independent of its catalytic activity but requires nuclear localization. *PLoS ONE*, *8*(7), e70062. https://doi.org/10.1371/journal.pone.0070062.
40. Mandal, S., Mandal, A., Johansson, H. E., Orjalo, A. V., & Park, M. H. (2013). Depletion of cellular polyamines, spermidine and spermine, causes a total arrest in translation and growth in mammalian cells. *Proceedings of the National Academy of Sciences*, *110*(6), 2169–2174. https://doi.org/10.1073/pnas.1219002110.
41. Nisenberg, O., Pegg, A. E., Welsh, P. A., Keefer, K., & Shantz, L. M. (2006). Overproduction of cardiac S-adenosylmethionine decarboxylase in transgenic mice. *Biochemistry Journal*, *393*(1), 295–302. https://doi.org/10.1042/BJ20051196.
42. Shi, C., Welsh, P. A., Sass-Kuhn, S., Wang, X., McCloskey, D. E., Pegg, A. E., & Feith, D. J. (2012). Characterization of transgenic mice with overexpression of spermidine synthase. *Amino Acids*, *42*(2-3), 495–505. https://doi.org/10.1007/s00726-011-1028-6.
43. Chang, Y. C., Su, C. Y., & Hsiao, M. (2016). Therapeutic targeting of methylthioadenosine phosphorylase. *Cancer Cell & Microenvironment*, *3*(3), e1322. https://doi.org/10.14800/ccm.1322.
44. Borrego, S. L., Fahrmann, J., Datta, R., Stringari, C., Grapov, D., Zeller, M., Chen, Y., Wang, P., Baldi, P., Gratton, E., Fiehn, O., & Kaiser, P. (2016). Metabolic changes associated with methionine

stress sensitivity in MDA-MB-468 breast cancer cells. *Cancer & Metabolism*, *4*, 9. https://doi.org/10.1186/s40170-016-0148-6.
45. Cavuoto, P., & Fenech, M. F. (2012). A review of methionine dependency and the role of methionine restriction in cancer growth control and life-span extension. *Cancer Treatment Reviews*, *38*(6), 726–736. https://doi.org/10.1016/j.ctrv.2012.01.004.
46. Guo, H. Y., Herrera, H., Groce, A., & Hoffman, R. M. (1993). Expression of the biochemical defect of methionine dependence in fresh patient tumors in primary histoculture. *Cancer Research*, *53*, 2479–2483.
47. Wanders, D., Hobson, K., & Ji, X. (2020). Methionine restriction and cancer biology. *Nutrients*, *12*(3), 684. https://doi.org/10.3390/nu12030684.
48. Ashkavand, Z., O'Flanagan, C., Hennig, M., Du, X., Hursting, S. D., & Krupenko, S. A. (2017). Metabolic Reprogramming by Folate Restriction Leads to a Less Aggressive Cancer Phenotype. *Molecular Cancer Research*, *15*, 189–200. https://doi.org/10.1158/1541-7786.MCR-16-0317.
49. Song, Y. H., Shiota, M., Kuroiwa, K., Naito, S., & Oda, Y. (2011). The important role of glycine N-methyltransferase in the carcinogenesis and progression of prostate cancer. *Modern Pathology*, *24*(9), 1272–1280. https://doi.org/10.1038/modpathol.2011.76.
50. Ottaviani, S., Brooke, G. N., O'Hanlon-Brown, C., Waxman, J., Ali, S., & Buluwela, L. (2013). Characterisation of the androgen regulation of glycine N-methyltransferase in prostate cancer cells. *Journal of Molecular Endocrinology*, *51*(3), 301–312. https://doi.org/10.1530/JME-13-0169.
51. Yoon, J. K., Kim, D. H., & Koo, J. S. (2014). Implications of differences in expression of sarcosine metabolism-related proteins according to the molecular subtype of breast cancer. *Journal of Translational Medicine*, *12*, 149. https://doi.org/10.1186/1479-5876-12-149.
52. Strmiska, V., Michalek, P., Lackova, Z., Guran, R., Krizkova, S., Vanickova, L., Zitka, O., Stiborova, M., Eckschlager, T., Klejdus, B., Pacik, D., Tvrdikova, E., Keil, C., Haase, H., Adam, V., & Heger, Z. (2019). Sarcosine is a prostate epigenetic modifier that elicits aberrant methylation patterns through the SAMe-Dnmts axis. *Molecular Oncology*, *13*(5), 1002–1017. https://doi.org/10.1002/1878-0261.12439.
53. Dekhne, A. S., Shah, K., Ducker, G. S., Katinas, J. M., Wong-Roushar, J., Nayeen, M. J., Doshi, A., Ning, C., Bao, X., Frühauf, J., Liu, J., Wallace-Povirk, A., O'Connor, C., Dzinic, S. H., White, K., Kushner, J., Kim, S., Hüttemann, M., Polin, L., Rabinowitz, J. D., & Matherly, L. H. (2019). Novel pyrrolo [3,2-d]pyrimidine compounds target mitochondrial and cytosolic one-carbon metabolism with broad-spectrum antitumor efficacy. *Molecular Cancer Therapeutics*, *18*(10), 1787–1799. https://doi.org/10.1158/1535-7163.MCT-19-0037.
54. Lien, E. C., Ghisolfi, L., Geck, R. C., Asara, J. M., & Toker, A. (2017). Oncogenic PI3K promotes methionine dependency in breast cancer cells through the cystine-glutamate antiporter xCT. *Science Signaling*, *10*(510), eaao6604. https://doi.org/10.1126/scisignal.aao6604.